Overview of Functional Magnetic Resonance Imaging

Gary H. Glover, PhD

KEYWORDS

• Functional magnetic resonance imaging • BOLD fMRI
• Challenges • Future of fMRI

Functional magnetic resonance imaging (fMRI) is a class of imaging methods developed to demonstrate regional, time-varying changes in brain metabolism.[1–3] These metabolic changes can be consequent to task-induced cognitive state changes or the result of unregulated processes in the resting brain. Since its inception in 1990, fMRI has been used in an exceptionally large number of studies in the cognitive neurosciences, clinical psychiatry/psychology, and presurgical planning (between 100,000 and 250,000 entries in PubMed, depending on keywords). The popularity of fMRI derives from its widespread availability (can be performed on a clinical 1.5 T scanner), noninvasive nature (does not require injection of a radioisotope or other pharmacologic agent), relatively low cost, and good spatial resolution. Increasingly, fMRI is being used as a biomarker for disease,[4,5] to monitor therapy,[6] or for studying pharmacologic efficacy.[7] Thus, it is of interest to review the contrast mechanisms, the strengths and weaknesses, and evolutionary trends of this important tool.

BASIS FOR FMRI

fMRI is of course based on MRI, which in turn uses nuclear magnetic resonance coupled with gradients in magnetic field[8] to create images that can incorporate many different types of contrast such as T1 weighting, T2 weighting, susceptibility, flow, and so forth.[9] To understand the particular contrast mechanism predominantly used in fMRI it is necessary to first discuss brain metabolism.

All the processes of neural signaling in the brain, including formation and propagation of action potentials, binding of vesicles to the presynaptic junction, the release of neurotransmitters across the synaptic gap, their reception and regeneration of action potentials in the postsynaptic structures, scavenging of excess neurotransmitters, and so forth, require energy in the form of adenosine triphosphate (ATP).[10] This nucleotide is produced principally by the mitochondria from glycolytic oxygenation of glucose, and its production results in carbon dioxide as a by-product. When a region of the brain is upregulated (ie, activated) by a cognitive task such as finger tapping, the additional neural firing and other increased signaling processes result in a locally increased energy requirement, in turn resulting in upregulated cerebral metabolic rate of oxygen ($CMRO_2$) in the affected brain region.[11] As the local stores of oxygen in tissues adjacent to capillaries are transiently consumed by glycolysis and waste products build up, various chemical signals (CO_2, NO, H^+) cause a vasomotor reaction in arterial sphincters upstream of the capillary bed, causing dilation of these vessels. The increased blood flow acts to restore the local [O_2] level required to overcome the transient deficit; however, for reasons that are still not fully understood more oxygen is delivered than is needed to offset the increase in $CMRO_2$. As a result, neural upregulation results initially in a buildup of deoxygenated hemoglobin

Supported by NIH Grant P41-RR009784.
The author has no conflicts to declare.
Department of Radiology, Stanford University, Lucas MRI Center, MC 5488, 1201 Welch Road, Stanford, CA 94305–5488, USA
E-mail address: gary.glover@stanford.edu

Neurosurg Clin N Am 22 (2011) 133–139
doi:10.1016/j.nec.2010.11.001
1042-3680/11/$ – see front matter

(Hb) and a decrease in oxygenated hemoglobin (HbO_2) in the intra- and extravascular spaces, followed within a second or two by a vasodilatory response that reverses the situation to result in an increase in [HbO_2] and decrease in [Hb] over that in the resting condition (**Fig. 1**).[12,13] This sequence of processes is described as the hemodynamic response to the neural event.

Thus, there are 2 primary consequences of increased neural activity, and both can be detected by MRI: increased local cerebral blood flow (CBF) and changes in oxygenation concentration (Blood Oxygen Level Dependent, or BOLD, contrast). The change in CBF can be observed using an injected contrast agent and perfusion-weighted MRI, first demonstrated by Belliveau and colleagues,[14] or noninvasively by arterial spin labeling (ASL).[15] However, ASL suffers from reduced sensitivity, increased acquisition time, and increased sensitivity to motion compared with the BOLD contrast method, and its use has therefore centered on obtaining quantitative measurements of baseline CBF for studies modeling the neurobiological mechanisms of activation[11,13] or calibration of vasoreactivity,[16] rather than in routine mapping of brain function.

The second mechanism, termed BOLD contrast, was first demonstrated in rats[17,18] and later in humans,[1–3,19] and is the contrast that is used in virtually all conventional fMRI experiments. BOLD contrast results from the change in magnetic field surrounding the red blood cells depending on the oxygen state of the hemoglobin. When fully oxygenated, HbO_2 is diamagnetic and is magnetically indistinguishable from brain tissue.

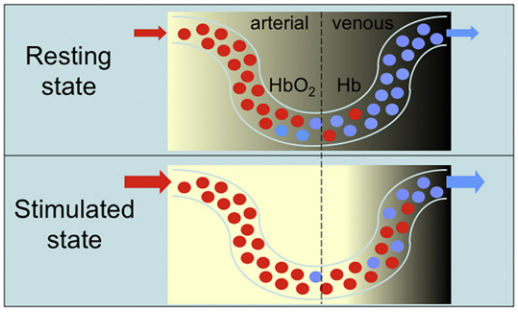

Fig. 1. Sketch of brain tissue containing a capillary during rest (*top*) and activation (*bottom*). Red and blue circles represent red blood cells that are fully oxygenated (HbO_2) and fully deoxygenated (Hb), respectively. The MRI signal is depressed in the venous side of the capillary due to the paramagnetic susceptibility of the Hb acting as an endogenous contrast agent (shown darker). In the stimulated condition, increased blood flow causes the Hb to be swept out and replaced by HbO_2, causing a BOLD signal increase.

However, fully deoxygenated Hb has 4 unpaired electrons and is highly paramagnetic.[20] This paramagnetism results in local gradients in magnetic field whose strength depends on the [Hb] concentration. These endogenous gradients in turn modulate the intra- and extravascular blood's T2 and T2* relaxation times through diffusion and intravoxel dephasing, respectively. Using a gradient refocused echo (GRE) MRI pulse sequence,[9] the acquisition is made sensitive to T2* and T2. At 1.5 T and 3 T, the T2* contrast is predominant and is largest in venules,[21] whereas at higher field strength the diffusion-weighted contrast of T2 relaxation becomes more important and, because signals are generated preferentially in capillaries and tissue with spin-echo acquisitions, provides greater spatial specificity.[22,23] Because most fMRI is currently performed at 3 T or below, BOLD fMRI uses primarily GRE methods because of the increased T2* contrast.[24]

Task activation fMRI studies seek to induce different neural states in the brain as the visual, auditory, or other stimulus is manipulated during the scan, and activation maps are obtained by comparing the signals recorded during the different states. Therefore, it is important to collect each image in a snapshot mode to avoid head motion, and prevent physiologic processes of respiration[25] and cardiovascular functions[26,27] from injecting noise signals unrelated to the neural processing being interrogated. In general, most fMRI is performed using an echo planar imaging (EPI) method,[28] which can collect data for a 2-dimensional image in approximately 60 milliseconds at typical resolutions ($3.4 \times 3.4 \times 4$ mm^3 voxel size). Whole brain scans with approximately 32 2-dimensional slices typically are acquired with a repetition time (TR) of 2 seconds per volume. Each voxel in the resulting scan produces a time series that is subsequently analyzed in accordance with the task design.

THE FMRI EXPERIMENT

The typical fMRI task activation experiment uses visual, auditory, or other stimuli to alternately induce 2 or more different cognitive states in the subject, while collecting MRI volumes continuously as already described. With a 2-condition design, one state is called the experimental condition and the other is denoted the control condition; the goal is to test the hypothesis that the signals differ between the 2 states. Using a block design, the trials are arranged to alternate between the experimental and control conditions, as shown in **Fig. 2**, with each block typically being a few tens of seconds long. The block design is optimum

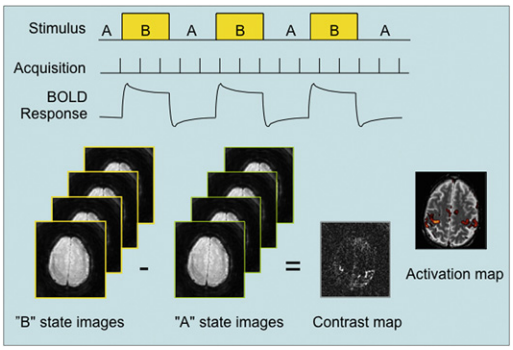

Fig. 2. Block-design fMRI experiment. A neural response to the state change from A to B in the stimulus is accompanied by a hemodynamic response (as shown in **Fig. 1**) that is detected by the rapid and continuous acquisition of MR images sensitized to BOLD signal changes. Using single or multivariate time series analysis methods, the average signal difference between the 2 states is computed for the scan and a contrast map generated. A statistical activation map is finally obtained using a suitable threshold for the difference; the map depicts the probability that a voxel is activated, given the uncertainty due to noise and the small BOLD signal differences.

for detecting activation, but a jittered event-related (ER) design is superior when characterization of the amplitude or timing of the hemodynamic response is desired.[29,30] In the ER design, task events are relatively brief and occur at nonconstant intertrial intervals with longer periods of control condition, which allows the hemodynamic response to return more fully to baseline. Jittering the timing serves to sample the hemodynamic response with higher temporal frequency in the overall time series, but may also be used to induce a desired cognitive strategy, for example, to avoid an anticipatory response or maintain attention.

The degree to which valid inferences can be drawn from the measured time series data depends in large part on careful design of the task. The investigator must take care that only the effect of interest changes between experimental and control conditions, while confounding effects such as attention and valence are maintained constant or irrelevant. In some studies this is straightforward, such as in the use of a sensory task for presurgical mapping, where the goal is only to localize activation so that important brain functions can be maintained after surgery. In this case the signal intensity is of minor interest as long as it is adequate to characterize the functional substrates to be preserved during surgical intervention. In many other cases, however, comparative inferences are desired, such as in parametric studies of the influence of task difficulty on a cognitive process, and thus control of such factors as learning, adaptation, and salience must be considered.

ANALYSIS METHODS

Once the images have been acquired, the time series data must be processed to obtain maps of brain activation. Because the BOLD contrast is small (<1% in many studies of higher cognitive processes),[31] simply averaging images over the experimental and control conditions and then subtracting (as sketched in **Fig. 2**) is inadequate to reliably determine differences because noise will compete to render false positives and negatives. The noise results from thermal sources in the subject and electronics, bulk motion of the head, cardiac and respiratory-induced noise, and variations in baseline neural metabolism. Because the noise can sometimes be larger than the signal of interest, fMRI analyses compare the signal difference between the states using a statistical test. These tests result in an activation map that is a function of the probability that the brain states differ. The statistical test for activation can use a general linear model,[32,33] cross-correlation with a modeled regressor,[34] or one of several data-driven approaches such as independent components analysis.[35] The models against which the acquired data are tested include the experimental design of interest as well as "nuisance regressors" of no interest such as signal drift, motion, and noise reflected in global or white-matter signals. In all cases, the activation testing is preceded by a series of preprocessing steps.

The steps in preprocessing can include all or some of the following: (1) time-slice correction, to eliminate differences between the time of acquisition of each slice in the volume; (2) motion coregistration, in which affine head motion is detected and the time series of volumes is resampled to register each time frame to a reference frame, such as the first or middle time series point; (3) correction for physiologic noise from breathing and cardiovascular function,[25,26] low pass and/or high pass temporal filtering to improve the statistics while removing spectral components of no interest; (4) spatial smoothing to improve the signal to noise ratio (SNR) and improve the normality of the noise distribution; (5) prewhitening to correct for autocorrelation in the time series.[31] The analysis of fMRI data continues to be a subject of intense research at this time, and is one about which numerous books have been written, to which the reader is referred for further information (eg, Sarty[36]).

COMPARISONS WITH OTHER FUNCTIONAL IMAGING MODALITIES

fMRI can be compared with other imaging methods used to obtained functional assessment of brain metabolism in terms of spatial and temporal resolution and availability. The primary alternatives are positron emission tomography (PET), near-infrared spectroscopy (NIRS), electroencephalography (EEG), and magnetoencephalography (MEG).[31]

Spatial Resolution

Resolution in fMRI is limited primarily by SNR because of the necessity for rapid acquisition of time series information. For MRI, $SNR \propto p^2 w \sqrt{T_{acq} N}$, where p is the pixel size, w the slice thickness, T_{acq} is the k-space readout time, and N the number of time frames. Thus, as T_{acq} is reduced for single-shot imaging (typically 20–30 milliseconds) the pixel size must be increased over that for conventional anatomic imaging to maintain an acceptable SNR. Accordingly, the typical fMRI pixel size is 3 to 4 mm, although with higher field magnets (7 T) a pixel size of 500 μm or less may be readily achieved.[22] The resolution of PET is limited by the size of the gamma-ray detectors as well as the positron-electron annihilation range, and is typically 5 to 10 mm or more. NIRS resolution is low (10–20 mm) and is limited predominantly by the strong scatter and attenuation of infrared photons (which also limits the depth of cortex that can be imaged within a banana-shaped region connecting optodes), the modest density of optodes, and the ill-conditioned inverse problem of reconstructing 3-dimensional maps of [Hb] from scalp recordings.[37] The resolution in EEG and MEG is similarly limited to greater than 10 to 20 mm by the fact that a unique reconstruction of dipoles is not possible from scalp-based measurements of electrical or magnetic distributions and models, and regularization must be employed for model estimation. Unlike EEG, MEG does not have the confounding factor that scalp recordings may be spatially distorted by heterogeneous electrical conduction paths within the brain/skull.

Temporal Resolution

Temporal resolution of fMRI is limited by hemodynamic response time; typically the BOLD response has a width of ~3 seconds and a peak occurring approximately 5 to 6 seconds after the onset of a brief neural stimulus. This rate is much slower than the underlying neural processes, and temporal information is thereby heavily blurred. Nevertheless, by jittering ER stimuli and using appropriate analysis methods,[29] temporal inferences in the 100-millisecond resolution range can be achieved.[38] PET scans require minutes to complete because of the low count rates of injected radionuclides, so changes in neural processes can only be studied by repeated scanning. Like BOLD, NIRS reports changes in blood oxygenation and, exacerbated by low SNR of near-infrared photons in the brain, has temporal limitations similar to those of fMRI. EEG and MEG, on the other hand, have millisecond temporal resolution and can easily capture the dynamics of evoked responses that last a few milliseconds to several hundred milliseconds. Multimodal approaches combining fMRI and EEG use fMRI maps as spatial priors to reconstruct high temporal resolution electrophysiology, thereby gaining resolution in both dimensions.[39]

STRENGTHS AND WEAKNESSES OF FMRI

From the foregoing discussion, a primary strength of fMRI is its relatively high spatial resolution and availability. In addition, it is readily available to both clinical and academic researchers, is noninvasive, and can provide high-resolution anatomic scans in the same session to use for localization, vessel identification,[40] or development of maps of white matter connectivity through the use of diffusion tensor imaging.[41]

Because BOLD contrast derives from the sluggish hemodynamic response to metabolic changes, a significant weakness is its low temporal resolution. Another problem is signal dropout and/or spatial distortion in frontal orbital and lateral parietal regions, caused by the difference of approximately 9 ppm in magnetic susceptibility at interfaces between air and brain tissue.[42] This situation can result in erroneous lack of BOLD signal in ventral, temporal, and prefrontal cortex regions important in many cognitive studies. Many methods have been developed to diminish these susceptibility losses, although most involve some trade-off of SNR in magnetically uniform brain regions.[42–48] Other weaknesses include the scanner's loud noise associated with switched magnetic fields, which can cause confounding factors in studies of audition[49,50] and resting state networks[51]; however, methods using interleaved scanning/stimulus delivery epochs can avoid these problems, albeit with some loss of flexibility in experimental design.[49,52] Finally, the high magnetic fields require customized stimulus delivery and subject response systems, again limiting flexibility and complicating multimodal experiments such as concurrent EEG recording.

FUTURE OF FMRI

For the most part, the MRI physics and technology development behind BOLD fMRI acquisitions are mature, and the trade-offs between acquisition speed, resolution, SNR, signal dropout, and contrast are well understood. Over the years, several investigators have attempted to develop alternatives to BOLD contrast using direct neural current detection,[53] although by now it is understood[54] that the weak size of the neural current signal relative to physiologic noise makes a breakthrough unlikely. Another alternative is the use of diffusion-weighted imaging to demonstrate activation-related changes in populations of bound versus free water distributions.[55,56] A potential advantage is that such diffusion-related changes may have more rapid responses than BOLD methods. However, again the signals are weaker than BOLD contrast and their biophysical origin is still unclear.[57] Other experiments have reported the use of spin echo rather than gradient echo acquisitions of BOLD contrast, especially at higher fields where T2* is foreshortened.[22]

While a modest research effort will continue in improving acquisition technology, the bulk of research in the development of fMRI has shifted to its application to answering more complex questions in cognitive neuroscience. One promising area is that of using activation maps as input to classification and state change algorithms to predict or classify cognitive behavior, such as predicting brain states[58,59] (also see, eg, Norman and colleagues[60] for a review). Other emerging uses of fMRI include the development of quantitative measures, that is, biomarkers for disease or monitoring behavioral modification such as reading disorders. A cautionary note, however, is that because of the small BOLD responses typical of cognitive processes, most studies are limited to employing group statistics to make inferences about populations rather than about individuals. Thus the use of fMRI in quantifying individual characteristics may continue to be limited to those tasks for which relatively strong BOLD responses are observed, such as primary sensory systems. Resting state networks and their modification by disease conditions such as Alzheimer disease, depression, and other psychiatric disorders[61] are gaining attention. However, there is growing awareness that these networks may be much more complex in their spatiotemporal dynamics than previously thought,[62] and much more work is indicated to understand their role and utility in predicting individual behavior/physiology. Finally, feedback derived from real-time fMRI has been shown to allow subjects to learn pain-reduction strategies,[63] to enhance sensorimotor control,[64] and to control relevant brain regions in mood disorder experiments.[59] The reader is also referred to Bandettini[65] for additional considerations regarding the future of fMRI.

SUMMARY

Functional MRI has enjoyed an exciting development course with an exponential growth in published studies since its inception in the early 1990s, and it has become commonplace for clinical uses such as presurgical planning, fundamental cognitive neuroscience investigations, behavior modification, and training. Informed by fMRI, more sophisticated modeling of brain networks is certain to lead to new levels of understanding of the human brain.

ACKNOWLEDGMENTS

The author is indebted to C.E. Chang for suggestions on the manuscript.

REFERENCES

1. Bandettini PA, Wong EC, Hinks RS, et al. Time course EPI of human brain function during task activation. Magn Reson Med 1992;25:390.
2. Kwong KK, Belliveau JW, Chesler DA, et al. Dynamic magnetic resonance imaging of human brain activity during primary sensory stimulation. Proc Natl Acad Sci U S A 1992;89:5675.
3. Ogawa S, Lee TM, Kay AR, et al. Brain magnetic resonance imaging with contrast dependent on blood oxygenation. Proc Natl Acad Sci U S A 1990;87:9868.
4. Greicius MD, Srivastava G, Reiss AL, et al. Default-mode network activity distinguishes Alzheimer's disease from healthy aging: evidence from functional MRI. Proc Natl Acad Sci U S A 2004;101:4637.
5. Kim DI, Sui J, Rachakonda S, et al. Identification of imaging biomarkers in schizophrenia: a coefficient-constrainedindependent component analysis of the mind multi-siteschizophrenia study. Neuroinformatics 2010;8(4):213–29.
6. Richards TL, Berninger VW. Abnormal fMRI connectivity in children with dyslexia during a phoneme task: before but not after treatment. J Neurolinguistics 2008;21:294.
7. Wise RG, Preston C. What is the value of human FMRI in CNS drug development? Drug Discov Today 2010;15:973–80.
8. Lauterbur PC. Image formation by induced local interactions. Examples employing nuclear magnetic resonance. Nature 1973;242:190.

9. Bernstein MA, King KF, Zhou XJ. Handbook of MRI pulse sequences. New York: Elsevier Press; 2004.
10. Roland PE. Brain activation. New York: John Wiley & Sons; 1993.
11. Buxton R, Frank L. A model for the coupling between cerebral blood flow and oxygen metabolism during neural stimulation. J Cereb Blood Flow Metab 1997;17:64.
12. Buxton RB, Wong EC, Frank LR. Dynamics of blood flow and oxygenation changes during brain activation: the balloon model. Magn Reson Med 1998;39: 855.
13. Davis TL, Kwong KK, Weisskoff RM, et al. Calibrated functional MRI: mapping the dynamics of oxidative metabolism. Proc Natl Acad Sci U S A 1998;95:1834.
14. Belliveau JW, Kennedy DJ, McKinstry RC, et al. Functional mapping of the human visual cortex by magnetic resonance imaging. Science 1991;254:716.
15. Detre JA, Leigh JS, Williams DS, et al. Perfusion imaging. Magn Reson Med 1992;23:37.
16. Bangen KJ, Restom K, Liu TT, et al. Differential age effects on cerebral blood flow and BOLD response to encoding: associations with cognition and stroke risk. Neurobiol Aging 2009;30:1276.
17. Ogawa S, Lee TM. Magnetic resonance imaging of blood vessels at high fields: in vivo and in vitro measurements and image simulation. Magn Reson Med 1990;16:9.
18. Ogawa S, Lee TM, Nayak AS, et al. Oxygenation-sensitive contrast in magnetic resonance image of rodent brain at high magnetic fields. Magn Reson Med 1990;14:68.
19. Ogawa S, Menon RS, Tank DW, et al. Functional brain mapping by blood oxygenation level-dependent contrast magnetic resonance imaging. A comparison of signal characteristics with a biophysical model. Biophys J 1993;64:803.
20. Thulborn KR, Waterton JC, Matthews PM, et al. Oxygenation dependence of the transverse relaxation time of water protons in whole blood at high field. Biochim Biophys Acta 1982;714:265.
21. Weisskoff RM, Zuo CS, Boxerman JL, et al. Microscopic susceptibility variation and transverse relaxation: theory and experiment. Magn Reson Med 1994; 31:601.
22. Shmuel A, Yacoub E, Chaimow D, et al. Spatio-temporal point-spread function of fMRI signal in human gray matter at 7 Tesla. Neuroimage 2007; 35:539.
23. Yacoub E, Van De Moortele PF, Shmuel A, et al. Signal and noise characteristics of Hahn SE and GE BOLD fMRI at 7 T in humans. Neuroimage 2005;24:738.
24. Boxerman JL, Bandettini PA, Kwong KK, et al. The intravascular contribution to fMRI signal change: Monte Carlo modeling and diffusion-weighted studies in vivo. Magn Reson Med 1995;34:4.
25. Birn RM, Smith MA, Jones TB, et al. The respiration response function: the temporal dynamics of fMRI signal fluctuations related to changes in respiration. Neuroimage 2008;40:644.
26. Chang C, Cunningham JP, Glover GH. Influence of heart rate on the BOLD signal: the cardiac response function. Neuroimage 2009;44:857.
27. Chang C, Glover GH. Relationship between respiration, end-tidal CO(2), and BOLD signals in resting-state fMRI. Neuroimage 2009;47:1381–93.
28. Mansfield P. Multi-planar image formation using NMR spin echoes. J Phys Chem C 1977;10:L55.
29. Buckner RL, Bandettini PA, O'Craven KM, et al. Detection of cortical activation during averaged single trials of a cognitive task using functional magnetic resonance imaging. [see comments]. Proc Natl Acad Sci U S A 1996;93:14878.
30. Liu TT, Frank LR. Efficiency, power, and entropy in event-related FMRI with multiple trial types. Part I: theory. Neuroimage 2004;21:387.
31. Huettel SA, Song AW, McCarthy G. Functional magnetic resonance imaging. Sunderland (MA): Sinauer Associates, Inc; 2004.
32. Friston KJ, Holmes AP, Poline JB, et al. Analysis of fMRI time-series revisited. Neuroimage 1995; 2:45.
33. Worsley KJ, Liao CH, Aston J, et al. A general statistical analysis for fMRI data. Neuroimage 2002;15:1.
34. Bandettini PA, Jesmanowicz A, Wong EC, et al. Processing strategies for time-course data sets in functional MRI of the human brain. Magn Reson Med 1993;30:161.
35. Calhoun VD, Adali T, Pearlson GD, et al. A method for making group inferences from functional MRI data using independent component analysis. Hum Brain Mapp 2001;14:140.
36. Sarty GE. Computing brain activity maps from fMRI time series images. Cambridge (UK): Cambridge University Press; 2007.
37. Cui X, Bray S, Bryant DM, et al. A quantitative comparison of NIRS and fMRI across multiple cognitive tasks. Neuroimage 2010. [Epub ahead of print]. PMID: 21047559.
38. Ogawa S, Lee TM, Stepnoski R, et al. An approach to probe some neural systems interaction by functional MRI at neural time scale down to milliseconds. Proc Natl Acad Sci U S A 2000;97:11026.
39. Dale AM, Halgren E. Spatiotemporal mapping of brain activity by integration of multiple imaging modalities. Curr Opin Neurobiol 2001;11:202.
40. Menon RS. Postacquisition suppression of large-vessel BOLD signals in high-resolution fMRI. Magn Reson Med 2002;47:1.
41. Basser PJ, Pajevic S, Pierpaoli C, et al. In vivo fiber tractography using DT-MRI data. Magn Reson Med 2000;44:625.

42. Cho ZH, Ro YM. Reduction of susceptibility artifact in gradient-echo imaging. Magn Reson Med 1992; 23:193.
43. Constable R, Spencer D. Composite image formation in Z-shimmed functional MR imaging. Magn Reson Med 1999;42:110.
44. Glover GH, Law CS. Spiral-in/out BOLD fMRI for increased SNR and reduced susceptibility artifacts. Magn Reson Med 2001;46:515.
45. Hsu JJ, Glover GH. Mitigation of susceptibility-induced signal loss in neuroimaging using localized shim coils. Magn Reson Med 2005;53:243.
46. Stenger VA, Boada FE, Noll DC. Three-dimensional tailored RF pulses for the reduction of susceptibility artifacts in T2*-weighted functional MRI. Magn Reson Med 2000;44:525.
47. Weiger M, Pruessmann KP, Osterbauer R, et al. Sensitivity-encoded single-shot spiral imaging for reduced susceptibility artifacts in BOLD fMRI. Magn Reson Med 2002;48:860.
48. Yang QX, Dardzinski BJ, Li S, et al. Multi-gradient echo with susceptibility inhomogeneity compensation (MGESIC): demonstration of fMRI in the olfactory cortex at 3.0 T. Magn Reson Med 1997;37:331.
49. Gaab N, Gabrieli JD, Glover GH. Assessing the influence of scanner background noise on auditory processing. I. An fMRI study comparing three experimental designs with varying degrees of scanner noise. Hum Brain Mapp 2007;28:703.
50. Gaab N, Gabrieli JD, Glover GH. Assessing the influence of scanner background noise on auditory processing. II. An fMRI study comparing auditory processing in the absence and presence of recorded scanner noise using a sparse design. Hum Brain Mapp 2007;28:721.
51. Gaab N, Gabrieli JD, Glover GH. Resting in peace or noise: scanner background noise suppresses default-mode network. Hum Brain Mapp 2008;29: 858.
52. Edmister WB, Talavage TM, Ledden PJ, et al. Improved auditory cortex imaging using clustered volume acquisitions. Hum Brain Mapp 1999;7:89.
53. Bodurka J, Bandettini PA. Toward direct mapping of neuronal activity: MRI detection of ultraweak, transient magnetic field changes. Magn Reson Med 2002;47:1052.
54. Luo Q, Gao JH. Modeling magnitude and phase neuronal current MRI signal dependence on echo time. Magn Reson Med 2010;64(6):1832–7.
55. Le Bihan D, Urayama S, Aso T, et al. Direct and fast detection of neuronal activation in the human brain with diffusion MRI. Proc Natl Acad Sci U S A 2006; 103:8263.
56. Li T, Song AW. Fast functional brain signal changes detected by diffusion weighted fMRI. Magn Reson Imaging 2003;21:829.
57. Miller KL, Bulte DP, Devlin H, et al. Evidence for a vascular contribution to diffusion FMRI at high b value. Proc Natl Acad Sci U S A 2007;104:20967.
58. Martinez-Ramon M, Koltchinskii V, Heileman GL, et al. fMRI pattern classification using neuroanatomically constrained boosting. Neuroimage 2006;31:1129.
59. Phan KL, Fitzgerald DA, Gao K, et al. Real-time fMRI of cortico-limbic brain activity during emotional processing. Neuroreport 2004;15:527.
60. Norman KA, Polyn SM, Detre GJ, et al. Beyond mind-reading: multi-voxel pattern analysis of fMRI data. Trends Cogn Sci 2006;10:424.
61. Greicius M. Resting-state functional connectivity in neuropsychiatric disorders. Curr Opin Neurol 2008; 21:424.
62. Chang C, Glover GH. Time-frequency dynamics of resting-state brain connectivity measured with fMRI. Neuroimage 2010;50:81.
63. deCharms RC, Maeda F, Glover GH, et al. Control over brain activation and pain learned by using real-time functional MRI. Proc Natl Acad Sci U S A 2005;102:18626.
64. deCharms RC, Christoff K, Glover GH, et al. Learned regulation of spatially localized brain activation using real-time fMRI. Neuroimage 2004;21:436.
65. Bandettini PA. What's new in neuroimaging methods? Ann N Y Acad Sci 2009;1156:260.